Physica Medica 64 (2019) 16–23

Contents lists available at ScienceDirect

Physica Medica

journal homepage: www.elsevier.com/locate/ejmp

Original paper

PET-CT post therapy dosimetry in radioembolization with resin ^{90}Y microspheres: Comparison with pre-treatment SPECT-CT ^{99m}Tc-MAA results

Elisa Richetta[a,*], Massimo Pasquino[a], Matteo Poli[a], Claudia Cutaia[a], Chiara Valero[a], Marco Tabone[b], Benedetta Peiretti Paradisi[c], Massimiliano Pacilio[d], Riccardo Emanuele Pellerito[e], Michele Stasi[a]

[a] Medical Physics Department, AO Ordine Mauriziano, Turin, Italy
[b] Gastroenterology Department, AO Ordine Mauriziano, Turin, Italy
[c] Energy Department, Politecnico di Torino, Italy
[d] Medical Physics Department, AOU Policlinico Umberto I, Rome, Italy
[e] Nuclear Medicine Department, AO Ordine Mauriziano, Turin, Italy

ARTICLE INFO

Keywords:
Radioembolization
Dosimetry
PET-TC
Microspheres

ABSTRACT

Resin microspheres radioembolization is an effective treatment for liver tumors when the surgical option is not feasible. Doses delivered to tumor and normal liver can be assess in the pre-therapy phase by means of a ^{99m}Tc-MAA SPECT-CT simulation and after the treatment with ^{90}Y PET-CT acquisition. The optimal therapeutic ^{90}Y activity is determined on ^{99m}Tc-MAA SPECT-CT dose results in order to avoid healthy parenchyma toxicity and to effectively irradiate the tumor. The assumption of identical radiopharmaceutical distribution between simulation and verification is still under debate and literature data showed controversial results. In this study 10 HCC patient's dosimetry performed on ^{99m}Tc SPECT-CT and ^{90}Y PET-CT were compared. Patients were selected when a good agreement between the pre and post-therapy distribution was observed in order to investigate the intrinsic dosimetric variations between the two imaging modalities. Mean doses (MIRD and Voxel approaches) showed a good correlation (Pearson's coefficient $r > 0.90$) both for tumor and normal liver. Dose Volume Histogram curves were compared with a good agreement particularly for normal liver (D50). Goal doses were achieved for 90% of patients. Bland-Altman analysis indicates lower variations for healthy parenchyma than for tumor (1.96 SD equal to 9.1 Gy and 68 Gy respectively) confirming the robustness of the dose-toxicity approach. PET-CT dosimetry well correlates with SPECT-CT doses (under assumption of same catheter position and ^{90}Y activity). Better agreement was showed for 7/10 and 8/10 patients for T and NL respectively, confirming dosimetry as effective tool to optimize and individualize the treatment.

1. Introduction

Radioembolization with microspheres is a minimally invasive therapy for non-resectable primary or metastatic liver tumors. Resin or glass ^{90}Y microspheres are infused through the hepatic artery assuming that tumor has a higher vascularization than the normal liver. In the past, when the technique was introduced, the choice of the activity to be administered to the patient was determined by means of empirical models, which did not take into account the tumor and non-tumor absorbed dose. A pitfall of the crudest, empirical method was 20 deaths in a single center. The procedure instead would have required a systematic 25% subjective reduction of activity prescribed with body surface area method as reported by Chiesa et al. [1]. On the contrary, data later published showed that local efficacy strongly correlates with tumor-absorbed dose and that the normal liver average absorbed dose is a toxicity risk factor. For these reasons a pre-therapy dosimetry becomes mandatory and it is achieved by a ^{99m}Tc-MAA (Macroaggregated Albumin) SPECT-CT acquisition simulating the ^{90}Y treatment. The dosimetry allows to estimate the dose to the tumor and the normal liver and to evaluate the best therapeutic ^{90}Y activity. This approach was thus implemented in many centers and its effectiveness was pointed out by several authors [2,3]. A European survey published in 2017 by the EANM Internal Dosimetry Task Force Report "Treatment Planning For Molecular Radiotherapy: Potential And Prospects" [4] reports that, in the year 2015, the pre-therapy dosimetry was performed on 82% of the treatments with resin and on 84% with glass.

* Corresponding author.
E-mail address: erichetta@mauriziano.it (E. Richetta).

https://doi.org/10.1016/j.ejmp.2019.05.025
Received 5 December 2018; Received in revised form 2 May 2019; Accepted 27 May 2019
Available online 19 June 2019

Post-therapy radioembolization dosimetry was initially performed on Bremsstrahlung images [5,6] acquired after the ^{90}Y administration. Quantitative imaging of Y-90 bremsstrahlung photons is challenging because of the continuous energy spectrum extending to 2.3 MeV. There is substantial downscatter that leads to poor contrast and the images have poor resolution because typically high energy collimators are used to reduce septal penetration by the higher energy photons [6]. For this reason, as reported by the EANM survey [4], the post-therapy dosimetry for radioembolization was performed only in 26% of the treatments. However, a post treatment dose verification is recommended to estimate the actual amount of radiation delivered to tumor and normal liver, as indicated by the European regulations (EU Directive 59/2013). Although most of ^{90}Y decays are β-emitting, 32 per million ^{90}Y decays result in internal pair production that can be imaged using conventional PET-CT. The possibility of acquiring a ^{90}Y image by means of a conventional PET-CT scan after a resin radioembolization was reported in 2009 [7] showing the possibility for this radionuclide to become fully theranostic (i.e., it demonstrates both therapeutic and diagnostic attributes). Quantitative assessments of ^{90}Y radioactivity in phantoms or patients is more accurate if Time-of-Flight (ToF) PET reconstruction is used, that demonstrates some advantages when compared to non-ToF PET imaging systems [8]. In recent years, the diffusion of ToF PET-CT scanners has encouraged the post ^{90}Y radioembolization dosimetry both with absolute quantification approach and with relative calibration method, as reported by published data [9,10].

The aim of this paper is to compare post-therapy dosimetry performed on ^{90}Y PET-CT images to SPECT-CT ^{99m}Tc-MAA pre-therapy mean dose results. Differences in the distribution of the radiotracer can be observed when pre-therapy ^{99m}Tc images are compared to ^{90}Y post-therapy ones [10]. The reasons of such differences may be attributed to a change in the vascularization occurred between simulation and treatment, to a different positioning of the catheter or to a different flow of the macroaggregates compared to the microspheres. For these reasons, we limited our study to the cases in which the distribution of the radiopharmaceutical was observed to be the same in pre and post-therapy phases. Under this assumption, it was possible to better pursue the intrinsic variations of the same dosimetric method on the two different radiotracers ^{99m}Tc-MAA and ^{90}Y, where differences in concentration (numbers of injected spheres) and size are present.

2. Material and methods

10 patients affected by Hepatocellular Carcinoma (HCC) and treated with ^{90}Y resin microspheres (Sirtex) between January and May 2018 were collected for the study (10 males, Child A, mean age 68 y, range 54 ÷ 85 y). Interventional radiological procedure was performed at Mauriziano Hospital of Turin using a standard catheter (4F) to selectively infuse the resin microspheres into a lobe of the liver (9 right lobe, 1 left lobe). During the angiography procedure, the catheter was placed in the same position both in the ^{99m}Tc-MAA simulation phase and in the ^{90}Y therapeutic administration (pre and post-therapy angiographic images were overlapped to estimate catheter position differences and a median distance of 4 mm was found, range 1 ÷ 7 mm). This led to a similar radiopharmaceutical injection for all of the 10 patients, as confirmed also by visually inspecting the SPECT-CT and PET-CT images. Under this assumption, dose comparisons were performed in order to investigate the differences in the dose results due to the different radioisotope and imaging modality. For 2 other patients, instead, the catheter was placed in a different position during the simulation phase and the treatment phase (position shift > 15 mm). For this reason, a different distribution was found in pre and post images and they were a priori excluded from the study. After the therapeutic administration of ^{90}Y (mean activity 1712 ± 518 MBq, range 763 ÷ 2500 MBq), patients were hospitalized at Nuclear Medicine Therapeutic Department for 48 h.

2.1. Pre-therapy dosimetry

The radioembolization was simulated by means of ^{99m}Tc-MAA (Macro Aggregate Albumin). The administration (158 ± 33 MBq) was performed by the interventional radiologist no more than 10 days before treatment, assuming that the macroaggregates reflect the same distribution of ^{90}Y microspheres. The simulation allows not only to verify the absence of lung and gastric shunt but also to know the distribution of tumor and normal liver in advance in order to evaluate the optimal ^{90}Y therapeutic activity. Within 30 min from the ^{99m}Tc-MAA administration, patient was moved from the interventional room to the Nuclear Medicine Diagnostic Department in which a SPECT-CT (Siemens Symbia IntevoT2) and a PET-CT (Philips IngenuityTF) operate. A Whole-Body and tomographic SPECT-CT were acquired (voxel size 4.8 mm, LEHR collimators, matrix 128x128, 20 s/views, 60 views). The images were reconstructed by means of an iterative algorithm (Flash3D, 8 iterations, 8 subset, IRR Iterative Resolution Recovery, no partial volume correction) and co-registered with the simultaneous CT acquisition to apply attenuation and scatter corrections (DEW). ^{99m}Tc SPECT-CT images were analyzed to define the VOI (Volume of Interest) of tumor (T) and normal liver (NL). The active part of the tumor lesion was inspected on the emissive SPECT-CT image and the volume compared to the diagnostic CT one (performed with contrast medium). Using a volumetric tool (Volumetrix Siemens) on the e.soft processing workstation, both volumes T (only the active part was considered as tumor) and NL (where the total active part of the treated lobe will be indicated as 'scintigraphic' NL) were countered. Lesion T was identified with a threshold method (mean 35%, range 27–40 %) in order to comprehend the active part of the tumor. For the scintigraphic NL, a threshold value was set to include all the uptaking part of the treated lobe (mean 3%, range 2–4%). Total counts for the two VOIs T and NL were obtained. Volumes for T and scintigraphic NL are reported in Table 1. The volume of the whole normal liver (including the non-treated lobe) was also measured on the CT image. Mean doses to tumor and normal liver were calculated to estimate the optimal therapeutic ^{90}Y activity in order to deliver less than 40 Gy to the whole normal liver (including the non-treated lobe) and, when possible, more than 150 Gy to the tumor. These dose limits are suggested by Strigari et al. [5] when resin microspheres are used.

2.2. Post-therapy dosimetry

A PET-CT scan (OSEM3D reconstruction algorithm, 3 iterations, 33 subsets, voxel size 4.0 mm, Time of Flight kernel 14.1 cm) was acquired to estimate the doses effectively delivered during the therapy. Resolution recovery, partial volume correction and absolute calibration for ^{90}Y quantitative activity measurements have not been used. Due to the very low β^+ branching ratio ($\sim 32 \times 10^{-6}$), the bed time acquisition was increased up to 20 min, in order to achieve acceptable image statistics. PET-CT images were subsequently corrected for scatter and attenuation. On the Philips processing workstation (IntelliSpace Portal 9.0), the VOIs for T and NL were contoured. The VOIs were copied from the SPECT-CT images and placed in the same position on the PET-CT images; then, a threshold method was applied for both T and NL to reproduce exactly the same volume values. The threshold values were set differently for each patient in order to obtain the same volume values for T and NL in the SPECT-CT pre-therapy phase.

2.3. Multi-compartmental MIRD dose method

Both for pre-therapy and post-therapy phases, mean dose to tumor and scintigraphic normal liver (the irradiated part of the healthy parenchyma) were calculated with MIRD multi-compartmental formulas [2,11,12].

The TLR (tumor-to-healthy-liver activity concentration ratio) was calculated; the lung shunting fraction (LSF) was calculated on SPECT-

Table 1
Volumes for tumor and normal liver as well as the percentage of Lung Shunt Fraction (LSF) are reported for SPECT-CT and PET-CT image results. The actual administered activity is shown too.

	Activity	Tumor [ml]		Normal Liver [ml]		LSF [%]	LSF [%]
Patient	[GBq]	SPECT-CT	PET-CT	SPECT-CT	PET-CT	SPECT-CT	PET-CT
Volumes and Lung Shunt Fraction (LSF)							
#1	2.0	20	21	1244	1294	1.5	0.5
#2	1.3	231	243	581	598	0.7	0.1
#3	1.8	47	48	1126	1182	1.8	0.3
#4	1.4	180	180	1970	1872	3.1	0.2
#5	0.8	64	64	371	442	2.2	0.4
#6	2.5	429	417	1271	1273	2.9	0.1
#7	2.3	214	218	1476	1527	2.4	0.1
#8	1.3	167	161	928	919	2.3	0.2
#9	2.0	127	120	1319	1284	4.2	0.1
#10	1.8	647	630	1441	1533	2.1	0.2
Mean	1.7	213	210	1173	1192	1.7	0.2
1STD	0.5	192	187	458	435	0.6	0.1

CT pre-therapy dosimetry images. In PET-CT acquisition, due to the long acquisition time (20 min/bed), only two beds were acquired to scan the liver region. The liver was placed in the lower part of the image in order to include also the largest possible portion of the lungs. For small size patients, lungs were completely scanned but for taller patients they were truncated in the upper part of the lung lobe. The LSF was calculated on SPECT-CT and PET-CT images on the same portion of the lungs.

Fractional uptake for the irradiated normal liver is

$$= (1 - LSF)\frac{mass_{normal\ \ liver}(g)}{mass_{tumor}(g) \times TLR + mass_{normal\ \ liver}(g)}$$

The mean dose delivered to the normal liver for a given administered ^{90}Y activity is:

$$Dose_{normal\ \ liver}(Gy) = \frac{activity_{90_Y}(GBq) \times 50 \times fractional\ \ uptake_{normal\ \ liver}}{mass_{normal\ \ liver}(g)} \quad (1)$$

The mean dose to the whole normal liver was calculated by re-scaling the dose delivered to the scintigraphic normal liver obtained with equation (1) to the whole healthy liver, including the non-treated lobe.

The fractional uptake for tumor is $= (1 - LSF)\frac{TLR \times mass_{tumor}(g)}{TLR \times mass_{tumor}(g) + mass_{liver}}$

The mean dose delivered to the tumor is:

$$Dose_{tumor}(Gy) = \frac{activity_{90_Y}(GBq) \times 50 \times fractionaluptake_{tumor}}{mass_{tumor}(g)} \quad (2)$$

2.4. Voxel dose method

The MIRD multi-compartmental approach assumes a uniform distribution of the radiotracer (^{99m}Tc or ^{90}Y). It is however possible that the uptake of tumor and normal liver is not uniform due to the different vascularization of the microspheres. This can be observed by visually inspecting SPECT-CT and PET-CT images, where non-homogeneous radiopharmaceutical distribution is often evident.

In order to take these inhomogeneities into account, a voxel dosimetric approach needs to be followed [13]. The voxel dose can thus be estimated with the formula

$$D_{voxel} = A_{voxel} x S_{voxel} \quad (3)$$

where A_{voxel}(MBq·s) is the voxel cumulated activity (i.e. the integral activity over the time) equal to

$$\widetilde{A}_{voxel} = 1.443\ A_{voxel}\ T_{1/2}(^{90}Y) \quad (4)$$

(A_{voxel} is the initial activity into a voxel and $T_{1/2}(^{90}Y)$ in the physical ^{90}Y half-life).

Since the total administered ^{90}Y activity (A_{liver}) is completely uptaken into the treated liver lobe, the activity into the single voxel can be derived through the following simple proportion (patient-relative calibration method):

$$A_{voxel} = \frac{A_{liver}}{C_{liver}} c_{voxel} \quad (5)$$

where C are the counts in the total liver and in the voxel. This simple approach, called relative calibration method, do not require an absolute activity PET-CT scanner calibration.

Also for the voxel dose method, the LSF was taken into account subtracting from the A_{liver} the fraction of the lungs. S_{voxel} (mGy/MBq·s) factors were simulated with Monte Carlo [14] for the two different voxel sizes (SPECT-CT 4.8 mm, PET-CT 4.0 mm), considering the dose contribution deriving from the central voxel and the 3 adjacent voxels in the 3D plane. A MATLAB code was developed at our Medical Physics Department to perform the voxel dosimetry. The routine automatically imports and co-registers the SPECT-CT (or PET-CT images), converts the counts matrix into a cumulated activity matrix and finally, by multiplying each voxel for the S_{factor}, calculates a 3D dose matrix. On this matrix, the volumes for tumor and normal liver were defined through threshold or manual method (maintaining the same volume values employed with MIRD method). Mean dose for T and NL, as well as dose volume histogram (DVHs) curves, were obtained.

Mean doses (Gy) for tumor, scintigraphic normal liver and whole normal liver were compared in pre-therapy SPECT-CT and post-therapy PET-CT phase using a test for paired samples for both dosimetric methods (MIRD and voxel).

The correlation between pre-therapy and post-therapy dosimetry was investigated. The Bland-Altman plot was used to clinically confirm the agreement of the pre and post-therapy dosimetry. Finally, to take into account the different dose distribution in the VOIs, the Dose Volume Histogram (DVH) curves were compared in terms of D_{95}, D_{50} and D_5.

The actual administered activity to the patients was estimated. Patient's ^{90}Y vial was measured with a contaminameter (Berthold LB124) immediately before the therapy and after the injection (including the catheter, where a small amount of resin microspheres can be trapped), in order to estimate the residual activity. The actual administered activity values were used in the dosimetry calculation both in SPECT-CT and PET-CT dose calculations as reported in Table 1.

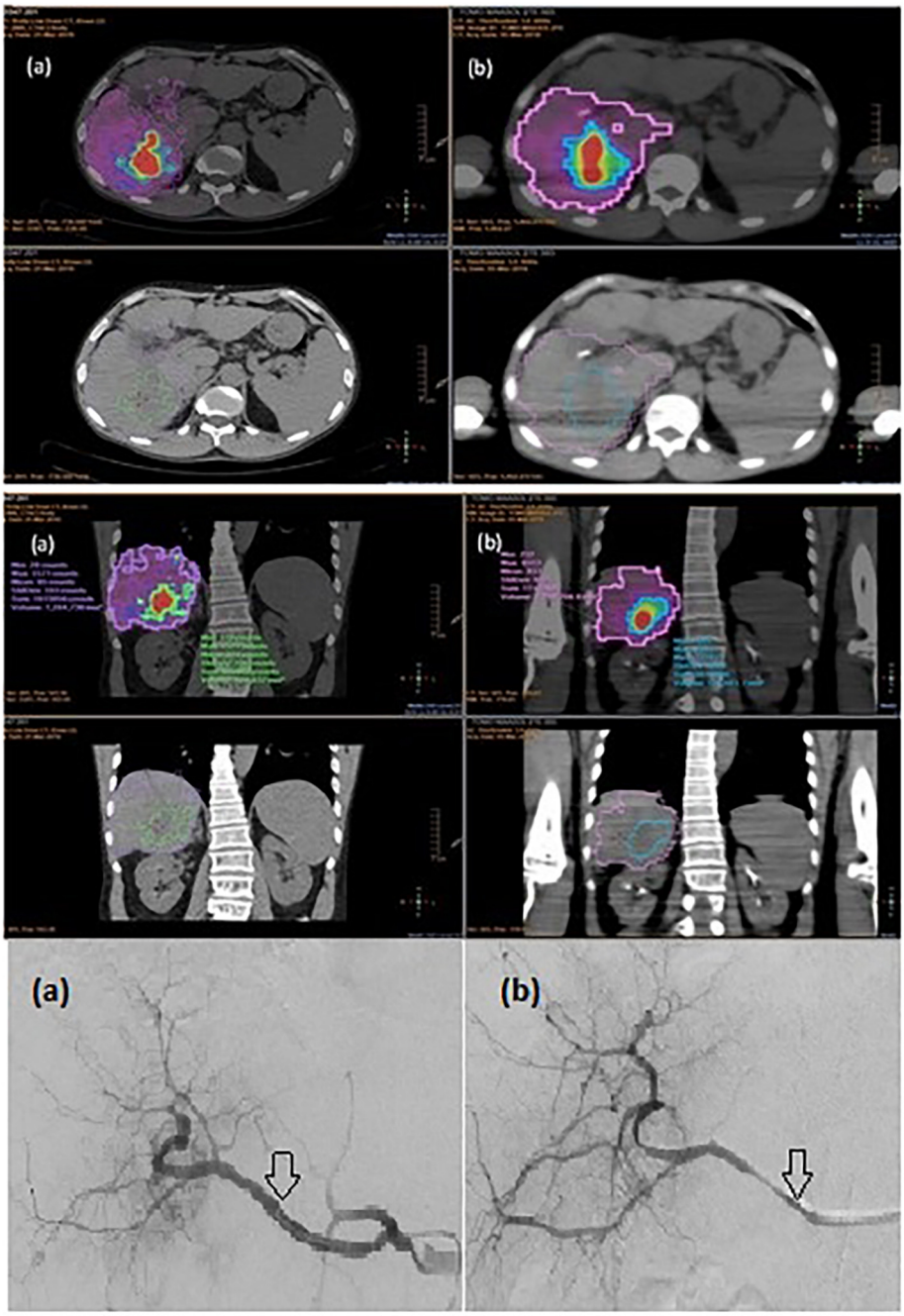

Fig. 1. ^{99m}Tc-MAA SPECT-CT images acquired for the pre-therapy dosimetry (a) and ^{90}Y PET-CT for post-therapy dosimetry after the radioembolization (b). In axial and coronal plane, fused emissive-CT and CT-only images are shown. Tumor and scintigraphic normal liver VOIs are reported. Angiographic images are shown.

3. Results

An example of activity of the hepatic lesion is reported on ^{99m}Tc-MAA SPECT-CT images for the pre-therapy phase (Fig. 1a) and on resin microspheres ^{90}Y PET-CT images for the post-therapy phase (Fig. 1b). The VOIs for tumor and normal liver are reported in axial and coronal planes both in emissive-CT fused images and CT-only images (patient #9). Angiographic images, where catheter positioning is evident (indicated by the arrow), are also reported. A visual comparison between the two different imaging techniques showed a similar radioisotope distributions into the lesion and the normal liver. Differences in local activity distribution are however visible, because of the different spatial resolution and the counts statistics of the two acquisition modalities. Such similar agreement was found for all of the 10 patients considered.

4. Volumes, lung shunt and administered activity

In Table 1, values of volumes for T and NL both for SPECT-CT and PET-CT are reported as well as Lung Shunt Fraction LSF (%) both for SPECT-CT and PET-CT. 3D tomographic images were employed for a more accurate estimation to avoid overestimation of planar lung shunt fraction as reported by literature [15]. The actual administered activity is reported; the percentage difference between the planned activity and the actual administered one was calculated (mean −3%, range −2 ÷ −4%).

4.1. Dose to tumor

Mean doses to tumor were 201.2 ± 79.4 Gy and 216.1 ± 100.4 Gy

Table 2
Mean doses [Gy] delivered to the tumor are reported for the 10 patients. MIRD and Voxel dose results are shown as well as the overall mean and standard deviation both for SPECT-CT and PET-CT. *p*-value of a *t*-test for paired sample is indicated in the last line when pre and post doses were compared within the same dosimetric method.

	MIRD method		Voxel method	
Patient	SPECT-CT	PET-CT	SPECT-CT	PET-CT
Tumor Mean Dose [Gy]				
#1	262.7	286.0	241.6	234.4
#2	205.5	158.6	214.4	173.4
#3	343.7	447.4	327.6	413.9
#4	172.3	178.8	170.1	173.9
#5	172.8	240.7	182.5	235.5
#6	128.3	144.0	147.9	158.1
#7	178.8	178.4	185.3	179.3
#8	228.9	204.2	229.0	199.2
#9	250.7	245.7	251.2	240.4
#10	67.9	76.8	83.2	82.4
Mean	201.2	216.1	203.3	209.1
1STD	79.4	100.4	79.4	85.9
p-value	0.30		0.64	

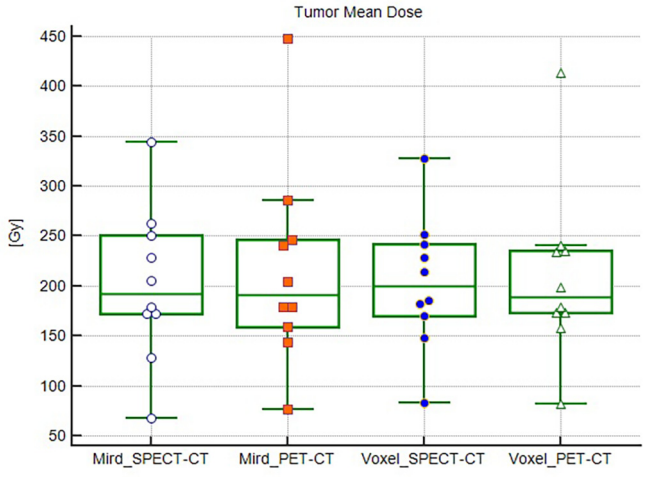

Fig. 2. Box-Plot of the tumor doses [Gy] is represented. Pre-therapy SPECT-CT and post-therapy PET-CT doses are plotted for the two dosimetric methods (MIRD and voxel): the single patient's values are represented as well as the mean value and the 25th–75th percentile range.

with MIRD method, 203.3 ± 79.4 Gy and 209.1 ± 85.9 Gy with Voxel method for SPECT-CT and PET-CT respectively. In Table 2, detailed dose data are reported and no significant difference was observed (*p*-value obtained from *t*-test for paired samples: MIRD 0.30, Voxel 0.64). The highest variations were found for patients #2, #3 and #5, while no particular discrepancies in catheter position were observed. Visually inspected images distributions of ^{90}Y resin microspheres were more inhomogeneous than ^{99m}Tc images, but no differences in simulation and therapeutic procedures were noticed. For 7/10 patients lower variations were found. In Fig. 2, dose values are graphically represented in a Box-Plot (25th and 75th percentile). 90% of the patients received a mean tumor dose higher than 150 Gy, corresponding to a Tumor Control Probability (TCP) equal to 1 for resin microspheres, as reported by Strigari et al. [5]. Only one patient (# 10) received a lower mean dose to the tumor equal to 82.4 Gy, corresponding to a lower TCP.

4.2. Dose to normal liver

Mean doses to the scintigraphic normal liver NL were

Table 3
Mean doses [Gy] delivered to the scintigraphic and whole normal liver are reported. For the 10 patients MIRD and Voxel dose results are shown as well as the overall mean and standard deviation both for SPECT-CT and PET-CT. *p*-value of a *t*-test for paired sample is indicated in the last line when pre and post doses were compared with the same dosimetric method.

	MIRD method		Voxel method	
Patient	SPECT-CT	PET-CT	SPECT-CT	PET-CT
Normal Liver (scintigraphic) Mean Dose [Gy]				
#1	75.2	71.8	71.5	65.0
#2	30.1	44.1	34.5	51.3
#3	63.9	59.2	62.7	55.9
#4	20.8	22.5	21.0	20.7
#5	72.9	51.9	76.4	48.4
#6	55.1	51.3	63.1	56.7
#7	51.0	49.7	53.2	50.0
#8	28.7	32.5	31.0	28.6
#9	51.5	55.8	52.2	55.0
#10	31.9	26.9	38.8	31.0
Mean	48.1	46.6	50.4	46.3
1STD	19.4	15.3	18.5	14.4
p-value	0.60	0.26		
Normal Liver (whole) Mean Dose [Gy]				
#1	40.50	40.22	38.50	36.38
#2	16.83	25.39	19.31	29.54
#3	53.91	52.41	52.92	49.49
#4	20.31	20.88	20.45	19.21
#5	13.29	11.28	13.93	10.52
#6	31.73	29.59	36.36	32.75
#7	29.30	29.53	30.57	29.74
#8	13.34	14.96	14.42	13.15
#9	41.06	43.31	41.62	42.74
#10	22.28	19.96	27.08	23.00
Mean	28.3	28.8	29.5	28.7
1STD	13.6	13.1	12.9	12.5
p-value	0.64	0.53		

48.1 ± 19.4 Gy and 46.6 ± 15.3 Gy with MIRD method, and 50.4 ± 18.5 Gy and 46.3 ± 14.4 Gy with Voxel method for SPECT-CT and PET-CT respectively. The mean doses to the whole normal liver, including the non-treated lobe, were 28.3 ± 13.6 Gy and 28.8 ± 13.1 Gy with MIRD method, 29.5 ± 12.3 Gy and 28.7 ± 12.5 Gy with Voxel method. In Table 3, detailed dose data are reported, as well as *t*-test for paired samples *p*-value (scintigraphic MIRD 0.60, voxel 0.23, whole normal liver MIRD 0.64, voxel 0.53) where no significant difference was observed. Patient #3 received a mean dose higher than the 40 Gy limit to the whole normal liver: this was accepted because of the small tumor size, the optimal condition of the surrounding healthy parenchyma, the absence of other lesions in the contralateral liver lobe and the aim of obtaining the down-staging to surgery for this specific case. For normal liver doses higher discrepancies were observed for patients #2 and #5; same consideration were reported for tumor results. In Fig. 3, dose values are graphically represented in a Box-Plot (25th and 75th percentile). 80% of patients received less than 40 Gy, corresponding to a normal-tissue complication probability (NTCP) to the whole normal liver equal to 0. Only 20% of patients exceeded this value, with a maximum dose of 53.9 Gy, corresponding to an NTCP of about 0.25 (95% CI) (Strigari et al. [5]).

A good correlation was found between SPECT-CT and PET-CT tumor doses (Pearson correlation coefficient *r*: MIRD 0.91, voxel 0.90) as well as normal liver doses (Pearson correlation coefficient *r*: MIRD 0.97, voxel 0.95). In Fig. 4, tumor and whole normal liver mean dose were plotted for voxel method. Similar results were found for MIRD method.

In order to evaluate the clinical impact of the dose differences on the clinical patient's management, the Bland-Altman analysis was performed. In Fig. 5, Bland-Altman plot is shown (for voxel dose results) both for whole normal liver (a) and tumor (b). For whole normal liver, the dose differences were found to be within +9.1 Gy and −7.4 Gy

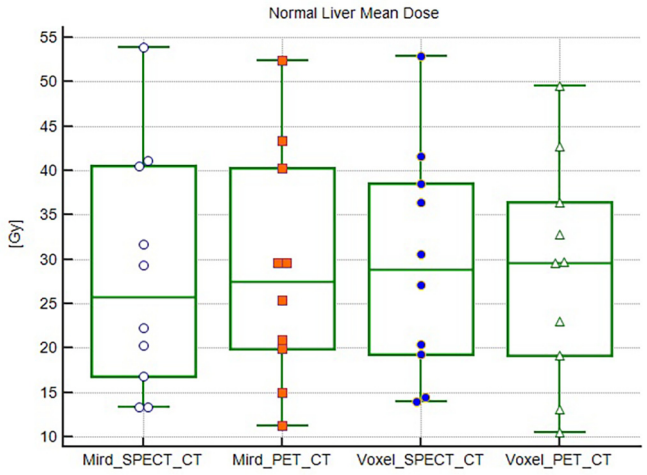

Fig. 3. Box-Plot of the whole normal liver doses [Gy] is represented. Pre-therapy SPECT-CT and post-therapy PET-CT doses are plotted for the two dosimetric methods (MIRD and voxel): the single patient's values are represented as well as the mean value and the 25th–75th percentile range.

(95% CI). These values, compared to the 40 Gy dose limit, correspond to a percentage difference of +22% and −18.5%. Higher differences were found on tumor dose within +68 Gy and −79 Gy corresponding to 32% and −38% of the mean dose delivered to the tumor (209 Gy in PET-CT voxel results).

In Fig. 6, an example of good agreement in DVHs curve (patient #9) and bad agreement (patient #1) is reported: the red curve represents the post-therapy PET-CT dosimetry and the blue curve represents the pre-therapy SPECT-CT dosimetry. Dose points D_{95}, D_{50}, D_5 for tumor and scintigraphic normal liver are also reported. In Table 4, (D_{PET}-D_{SPECT}) and percentage 100*(D_{SPECT}/D_{PET}-1) dose difference between SPECT-CT and PET-CT are reported for D_{95}, D_{50} and D_5, as well as mean, 1SD and p-value (*t*-test for paired samples between D_{SPECT} and D_{PET}). Lower discrepancies were found for D_{50} both for tumor and normal liver while higher differences were observed for D_{95}. D_5 in PET was higher than in SPECT in most patients (9/10).

5. Discussion

Dosimetry performed on SPECT-CT ^{99m}Tc-MAA pre-therapy images were compared to ^{90}Y PET-CT post-therapy images on a group of 10 patients. Mean dose as well as DVH curves were compared, but a 2D dose maps comparison is beyond our purpose, nor particle distribution variations or deviations between the activity planned and the activity actually administered were considered in this study. For all patients, the two arteriography procedures (simulation and therapy) were identical (similar catheter position) and a good agreement was found between pre and post-treatment mean dose to tumor and normal liver, both obtained with MIRD and Voxel approach (the same relative calibration method was applied both for pre-therapy SPECT-CT and post-therapy PET-CT to standardize the dosimetric method with the aim of dose comparisons). Analyzing these preliminary results, a similar catheter position during pre and post-therapy phase seems to favour a better dose agreemen, but it can be verified only a posteriori at the end of both procedures. A strong correlation (Pearson correlation coefficient) between pre and post-therapy dosimetry was achieved, suggesting that the previsional dosimetry (under above mentioned specific conditions) is a safe and useful predictor of the therapeutic treatment. The need for dosimetry in radioembolization is pointed out by many studies [2,13] but the effectiveness of ^{99m}Tc-MAA is still being debated. In a review paper, Garin (2016) summarized and discussed the available studies focused on MAA-based dosimetry [3] concluding that this approach is accurate (in HCC patients) and can be used in order to achieve a fully customized approach, including treatment intensification. Further studies are still necessary for the metastasis setting and in order to evaluate the maximal tolerated liver dose. Similar results were shown by Gnesin [9] where the partition model (MIRD) was applied on ^{99m}Tc-MAA SPECT-CT and compared to ^{90}Y ToF PET-CT doses on a group of 27 patients (HCC). The predicted-to-actual dose ratio (Gy/GBq) in pre and post-therapy phases showed a lower variation in normal liver compared to tumor dose results (especially for tumors larger than 150 ml). The predictive dosimetry based on ^{99m}Tc-MAA SPECT-CT is confirmed by the estimates of absorbed doses calculated on post-treatment ^{90}Y PET-CT for tumor and non tumor tissues. Moreover, the low variability of the NL dose demonstrates that pre-treatment dosimetry is particularly suitable for minimizing radiation-induced hepatotoxicity. Opposite conclusions were reported by Haste [10] in a recent study (2017). SPECT-CT and PET-CT images of 83 HCC patients treated with glass microspheres were analyzed in order to compare the absorbed dose to tumor and whole normal liver (WLNT). The ^{99m}Tc-MAA/^{90}Y limit of agreement was considered to be clinically acceptable only for WLNT (−15 to 15 Gy) and it was pointed out that catheter mismatch between ^{99m}Tc-MAA and ^{90}Y had a direct impact on absorbed dose mismatch between the 2 image sets. In this study Haste concluded that ^{99m}Tc-MAA was found to be a poor surrogate to quantitatively predict the subsequent ^{90}Y dose to hepatocellular tumors but ^{99m}Tc-MAA distribution correlated well with ^{90}Y distribution in the normal hepatic parenchyma. The differences in normal liver dose that we found in Bland-Altman analysis (−7.4 and 9.1 Gy) are comparable to Haste's results and confirm the effectiveness of the dosimetry based on the normal liver toxicity. In tumor analysis, we found a higher variation

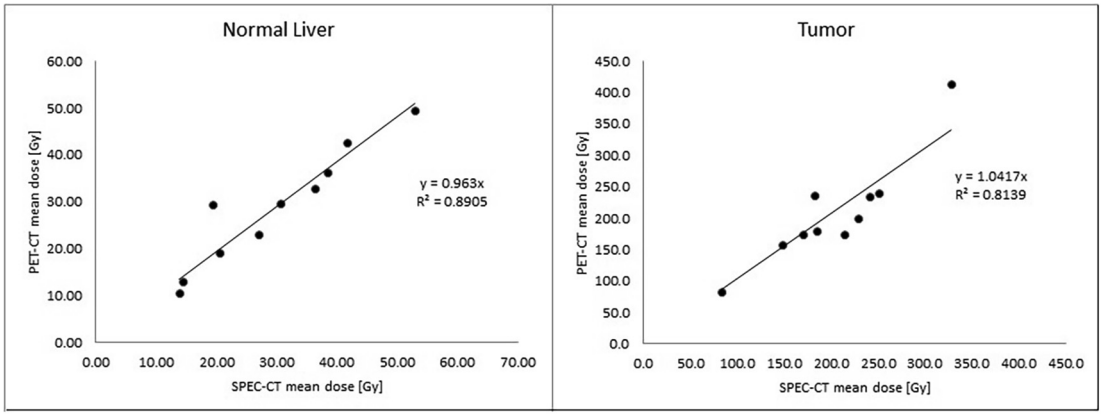

Fig. 4. In the graph, pre-therapy SPECT-CT mean dose [Gy] was plotted as function of PET-CT post-therapy dose [Gy] calculated with voxel method for tumor and whole normal liver. A linear fit equation is reported with the relative R^2 regression coefficient.

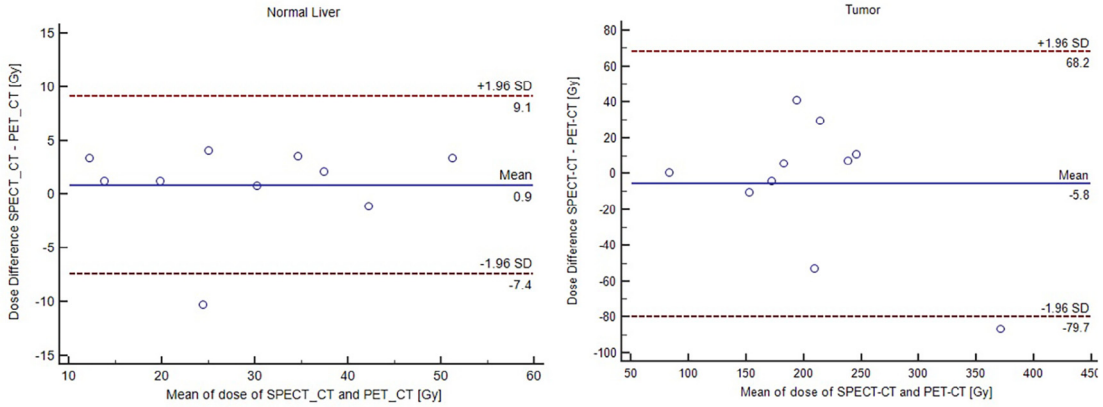

Fig. 5. Bland-Altman plots of tumor (a) and whole normal liver (b) represent the mean between SPECT and PET dose values [Gy] and the relative dose difference [Gy]. Voxel dose results were employed. The 1.96 SD interval is plotted (dotted line), indicating the 95% CI.

(+68 and −79 Gy) corresponding to a 38% percentage difference. These differences could be attributed to the different conditions between pre and post-therapy acquisition (time lapse, radiopharmaceutical and imaging techniques): the higher the local activity in tumor, the larger the variations. These dose differences should always be related to the treatment goal doses. Based on post therapy doses, 90% of the patients received a tumor dose higher than 150 Gy and 80% received a normal liver dose lower than 40 Gy. Analyzing pre-therapy dose results, these percentages become 80% for tumor and normal liver as well. Only 1 in 10 patients has had a different tumor dose result. For this reason, the patient management based on pre-therapy ^{99m}Tc SPECT-CT was correct for most of the enrolled patients (9/10). The analysis of the DVHs showed the local differences more precisely when point by point (D_{95},D_{50},D_5) curves comparisons were performed. Lower differences were found for D_{50} both for tumor and normal liver while D_{95} and D_5 showed higher variations. A more accurate analysis should compare SPECT-CT and PET-CT dose maps. Ferreira et al. [16] investigate the value of pre-treatment ^{99m}Tc-MAA SPECT-CT to predict intrahepatic ^{90}Y microspheres treatment dosimetry, using the gamma-index (γ-index) analytical method. γ-index passing rate values equal to 80% and greater than 90% were achieved for respectively conservative 10 mm/10% and less conservative 15 mm/15% (Distance To Agreement DTA/Dose Difference DD) tolerance criteria [16]. Radioembolization treatments performed in similar conditions give a γ-index passing rates (DTA/DD criteria) indicating the potential predictive power of dosimetry planning for post-radioembolization dosimetry outcome. To apply such a γ-index approach, attention should be paid to the dose maps co-registration methods

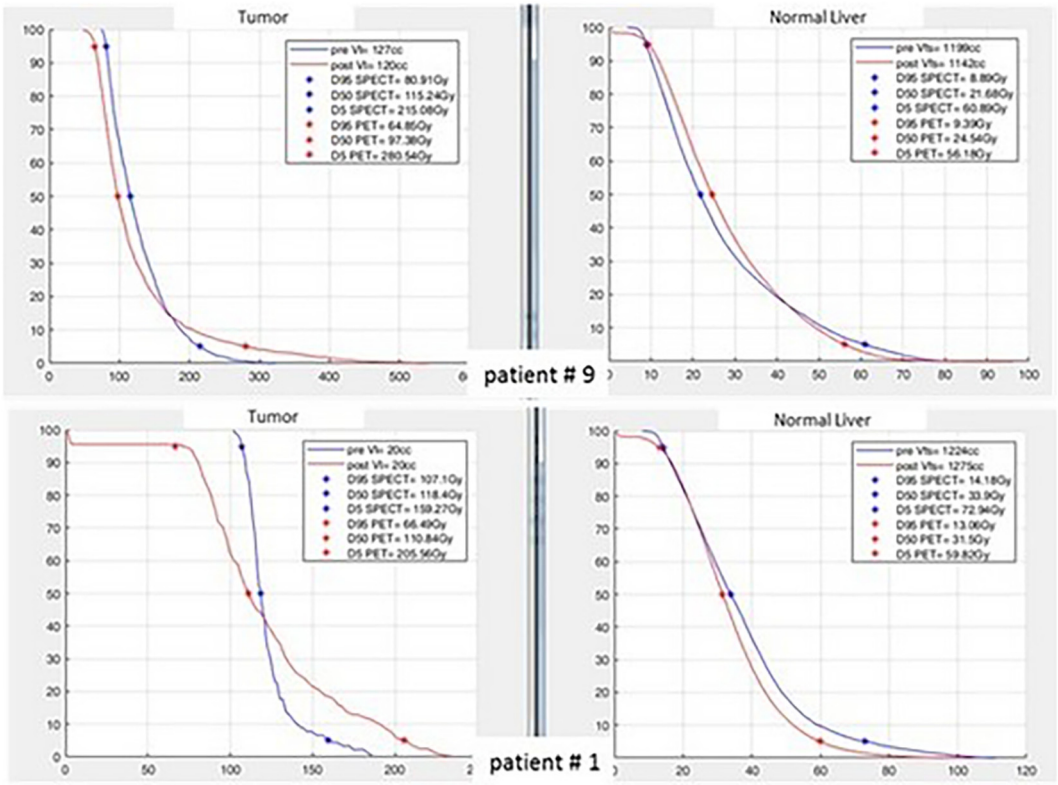

Fig. 6. Dose Volume Histogram curves are plotted for two patients: the red line represents the post-therapy dosimetry while the blue line represents the pre-therapy dosimetry. These results were obtained from the dose matrix calculated with the voxel method, imposing the same tumor and normal liver volumes in the SPET-CT and PET-CT phase. D_{95}, D_{50} and D_5 are reported.

Table 4
Dose difference [Gy] and percentage dose difference [%] are reported for the 10 patients for whom DVHs curves were compared point by point on specific dose levels (D_{95}, D_{50}, D_5). In the two last lines, mean and 1 standard deviation are indicated.

	Tumor			Normal Liver		
Patient	D95	D50	D5	D95	D50	D5
DVH dose difference [Gy]						
#1	−80	−15	86	−2	−5	−26
#2	11	−23	−150	1	18	21
#3	8	63	235	−3	−2	−31
#4	−19	5	17	−3	−1	2
#5	6	54	121	−17	−36	−6
#6	−4	8	42	−6	−11	1
#7	−13	−15	24	−8	−4	2
#8	−59	−45	52	−1	8	−43
#9	−32	−36	131	1	6	−9
#10	−79	−14	79	2	5	25
Mean	−26	−2	64	−4	2	−6
1STD	35	36	99	6	14	22
p-value	0.09	0.98	0.11	0.05	0.49	0.18
DVH percentage dose difference [%]						
#1	61	7	−21	9	8	22
#2	−10	14	48	−5	−39	−22
#3	−3	−17	−31	19	4	25
#4	31	−3	−5	46	4	−5
#5	−5	−24	−29	75	87	6
#6	4	−5	−17	29	19	−1
#7	11	9	−9	59	8	−2
#8	69	27	−12	29	−36	57
#9	25	18	−23	−5	−12	8
#10	58	15	−22	−5	−8	−23
Mean	24	4	−12	25	4	7
1STD	30	16	23	28	35	24

because a small spatial error could lead to a high dose difference. In the abdominal region, it can represent an issue because organ and respiratory motions are not negligible also when fiducial external markers or anatomical reference points are employed. This approach remains however promising and needs further investigations. This study was carried out on a small number of 10 patients; a larger cohort of patients is needed to confirm the agreement between pre-therapy SPECT-CT and Post-therapy PET-CT dose results. However, these preliminary results are still promising and could confirm the efficacy of the dosimetric approach in the liver radioembolization with resin microspheres.

6. Conclusions

Radioembolization can be safely simulated by a SPECT-CT ^{99m}Tc-MAA acquisition performed before the therapy to calculate the dose delivered to the tumor and to the healthy parenchyma. A good dose agreement (with a smaller variation for 7/10 patients and 8/10 for T and NL, respectively) was found on our patient dataset selected when the simulation and the therapeutic angiographic procedure were performed in an identical manner. This allows to predict the irradiation of the involved liver regions and to estimate the maximal ^{90}Y activity to be administered in order to give 40 Gy to the whole parenchyma and, if possible, more than 150 Gy to the lesion. After the therapeutic administration of ^{90}Y resin microspheres, a PET-CT ToF acquisition is useful to verify the dose delivered to tumor and normal liver. The good correlation between SPECT-CT and PET-CT dose confirms the feasibility of a patient specific dosimetry that is fundamental to individualize and optimize the treatment. A larger cohort of patients would be desirable to extend these preliminary dose results. However, other confounding effects (such as catheter positioning, time lapse) can affect the predictive effectiveness of the pre-therapy ^{99m}Tc SPECT-CT simulation and must be further investigated.

References

[1] Chiesa C, et al. Need, feasibility and convenience of dosimetric treatment planning in liver selective internal radiation therapy with (90)Y microspheres: the experience of the National Tumor Institute of Milan. Q J Nucl Med Mol Imaging 2011;55(2):168–97.

[2] Cremonesi, et al. Radioembolization of hepatic lesions from a radiobiology and dosimetric perspective. Front Oncol 2014;4(210). https://doi.org/10.3389/fonc.2014.00210. eCollection 2014.

[3] Garin, et al. Clinical impact of (99m)Tc-MAA SPECT/CT-based dosimetry in the radioembolization of liver malignancies with (90)Y-loaded microspheres. Eur J Nucl Med Mol Imaging 2016;43(3):559–75. https://doi.org/10.1007/s00259-015-3157-8. Epub 2015 Sep 4.

[4] Stokke, et al. Dosimetry-based treatment planning for molecular radiotherapy: a summary of the 2017 report from the Internal Dosimetry Task Force. EJNMMI Phys 2017;4(1). https://doi.org/10.1186/s40658-017-0194-3.

[5] Strigari L, et al. Efficacy and toxicity related to treatment of hepatocellular carcinoma with 90Y-SIR spheres: radiobiologic considerations. J Nucl Med 2010;51(9):1377–85. https://doi.org/10.2967/jnumed.110.075861. Epub 2010 Aug 18.

[6] Fabbri C, et al. Quantitative analysis of 90Y Bremsstrahlung SPECT-CT images for application to 3D patient-specific dosimetry. Cancer Biother Radiopharm 2009;24(1):145–54. https://doi.org/10.1089/cbr.2008.0543.

[7] Lhommel R, Goffette P, van den Eynde M, et al. Yttrium-90 TOF PET scan demonstrates high-resolution biodistribution after liver SIRT. Eur J Nucl Med Mol Imaging 2009;36(10):1696.

[8] Chadwick W. Theranostic imaging of yttrium-90. Biomed Res Int 2015;2015:1–11. https://doi.org/10.1155/2015/481279.

[9] Gnesin S, et al. Partition model-based 99mTc-MAA SPECT/CT predictive dosimetry compared with 90Y TOF PET/CT post treatment dosimetry in radioembolization of hepatocellular carcinoma: a quantitative agreement comparison. J Nucl Med 2016;57(11):1672–8. Epub 2016 Jun 15.

[10] Haste P, et al. Correlation of technetium-99m macroaggregated albumin and yttrium-90 glass microsphere biodistribution in hepatocellular carcinoma: a retrospective review of pretreatment single photon emission CT and posttreatment positron emission tomography/CT. J Vasc Interv Radiol 2017;28(5):722–730.e1. https://doi.org/10.1016/j.jvir.2016.12.1221. Epub 2017 Feb 24.

[11] Gallio E, et al. Calculation of tumour and normal tissue biological effective dose in 90Y liver radioembolization with different dosimetric methods. Phys Med 2016;32(12):1738–44. https://doi.org/10.1016/j.ejmp.2016.10.023. Epub 2016 Nov 18.

[12] Gulec SA, et al. Hepatic structural dosimetry in 90Y microsphere treatment: a Monte Carlo modeling approach based on lobular microanatomy. J Nucl Med 2010;51(2):301–10. https://doi.org/10.2967/jnumed.109.069278. Epub 2010 Jan 15.

[13] Chiesa C, et al. Radioembolization of hepatocarcinoma with 90Y glass microspheres: development of an individualized treatment planning strategy based on dosimetry and radiobiology. Eur J Nucl Med Mol Imaging 2015;42(11):1718–38. https://doi.org/10.1007/s00259-015-3068-8. Epub 2015 Jun 27.

[14] Laconelli N, et al. A free database of radionuclide voxel S values for the dosimetry of nonuniform activity distributions. Phys Med Biol 2012;57:517–53. https://doi.org/10.1088/0031-9155/57/2/517.

[15] Allred JD, et al. The value of 99mTc-MAA SPECT/CT for lung shunt estimation in 90Y radioembolization: a phantom and patient study. EJNMMI Res 2018;8:50. https://doi.org/10.1186/s13550-018-0402-8.

[16] Ferreira, et al. Patient-specific gamma-index analysis to evaluate 99mTc-MAA as a predictor for 90Y glass microspheres liver radioembolization dosimetry. Comp Methods Biomech Biomed Eng: Imag Visualiz 2017. https://doi.org/10.1080/21681163.2018.1501768.